

Quantum Gibbs ensemble Monte Carlo

Riccardo Fantoni and Saverio Moroni

Citation: *The Journal of Chemical Physics* **141**, 114110 (2014); doi: 10.1063/1.4895974

View online: <http://dx.doi.org/10.1063/1.4895974>

View Table of Contents: <http://scitation.aip.org/content/aip/journal/jcp/141/11?ver=pdfcov>

Published by the [AIP Publishing](#)

Articles you may be interested in

[Triplet correlations in the quantum hard-sphere fluid](#)

J. Chem. Phys. **123**, 104507 (2005); 10.1063/1.2009733

[Computation of the equation of state of the quantum hard-sphere fluid utilizing several path-integral strategies](#)

J. Chem. Phys. **121**, 3702 (2004); 10.1063/1.1776114

[Polymorphism in simple liquids: A Gibbs ensemble Monte Carlo study](#)

J. Chem. Phys. **120**, 8671 (2004); 10.1063/1.1698595

[Quantum Mode Coupling Theory and Path Integral Monte Carlo](#)

AIP Conf. Proc. **690**, 281 (2003); 10.1063/1.1632139

[A simulation study of the quantum hard-sphere Yukawa fluid](#)

J. Chem. Phys. **119**, 10256 (2003); 10.1063/1.1618731

The logo for AIP Applied Physics Letters is shown in a white, sans-serif font against a dark orange background. The letters 'AIP' are large, followed by a vertical bar and the text 'Applied Physics Letters'.

is pleased to announce **Reuben Collins**
as its new Editor-in-Chief



Quantum Gibbs ensemble Monte Carlo

Riccardo Fantoni^{1,a)} and Saverio Moroni^{2,b)}

¹*Dipartimento di Scienze Molecolari e Nanosistemi, Università Ca' Foscari Venezia, Calle Larga S. Marta DD2137, I-30123 Venezia, Italy*

²*DEMOCRITOS National Simulation Center, Istituto Officina dei Materiali del CNR and SISSA Scuola Internazionale Superiore di Studi Avanzati, Via Bonomea 265, I-34136 Trieste, Italy*

(Received 30 July 2014; accepted 8 September 2014; published online 18 September 2014)

We present a path integral Monte Carlo method which is the full quantum analogue of the Gibbs ensemble Monte Carlo method of Panagiotopoulos to study the gas-liquid coexistence line of a classical fluid. Unlike previous extensions of Gibbs ensemble Monte Carlo to include quantum effects, our scheme is viable even for systems with strong quantum delocalization in the degenerate regime of temperature. This is demonstrated by an illustrative application to the gas-superfluid transition of ⁴He in two dimensions. © 2014 AIP Publishing LLC. [<http://dx.doi.org/10.1063/1.4895974>]

I. INTRODUCTION

Monte Carlo (MC) simulations¹ in the Gibbs ensemble (GEMC) of Panagiotopoulos² have now been extensively used for several years to study first order phase transitions in classical fluids. According to the GEMC method, the simulation is performed in two boxes each of which contains one of two coexisting phases. Equilibration in each phase is guaranteed by moving particles within the respective box. Equality of pressures is satisfied in a statistical sense by expanding the volume of one of the boxes and contracting the volume of the other. Chemical potentials are equalized by transferring particles from one box to the other. This procedure avoids either the laborious search for matching free energies calculated separately for each phase, or the simulation of a system large enough to contain both phases and their interface.

Notwithstanding the isomorphism between quantum particles and classical ring polymers underlying the path integral formulation of quantum statistical physics,³ and the recognition that path integral Monte Carlo (PIMC) is a tremendously useful numerical tool⁴ to extract unbiased statistical properties of quantum systems, the development of Monte Carlo methods for quantum systems is more complex, and correspondingly less complete, than for classical ones. Putting aside the well known sign problem for fermions⁵ an important aspect is the development of methods able to simulate a given quantum system in different statistical ensembles.

Recently, a new approach to continuous space PIMC simulation was devised⁶ which makes use of the “Worm Algorithm” (WA) previously employed to study lattice models.⁷ The WA is formulated in an enlarged configuration space, which features the possible presence of an open world-line, the worm. It can simulate a system either in the grand canonical or the canonical ensemble, and it enjoys a favorable scaling of the computational cost with the system size for the calculation of properties related to the formation of long permutation cycles,⁸ such as the superfluid fraction or the one-body density matrix.

It is the purpose of the present work to exploit the WA⁶ to obtain an algorithm that is the full quantum analogue of the GEMC and thus can be used to study the gas-liquid phase transition of any (bosonic) quantum fluid.⁹ Several quantum generalizations of GEMC have appeared. However, some of them only consider particles which have internal quantum states but are otherwise classical;¹⁰ others¹¹ are limited to particles isomorph to relatively compact classical polymers (hence, high enough temperature and/or small enough quantumness); none of them features the structure of particle exchanges which underlies Bose (or Fermi) statistics. We apply the quantum Gibbs ensemble Monte Carlo (QGEMC) method to the liquid-gas coexistence of two-dimensional ⁴He where strong quantum effects, including superfluidity, are present.

II. CLASSICAL GIBBS ENSEMBLE MONTE CARLO

We begin with a brief summary of the Gibbs Ensemble Monte Carlo method that we deem useful for the subsequent quantum generalization. A detailed presentation is given in Ref. 12.

The system comprises a box of volume Ω_1 containing N_1 particles and a box of volume Ω_2 containing N_2 particles. The temperature T , the total number of particles $N = N_1 + N_2$, and the total volume $\Omega = \Omega_1 + \Omega_2$ are fixed, and there is no interaction between particles enclosed in different boxes. Starting from the partition function for the Gibbs ensemble

$$Z_G(N, \Omega, T) = \frac{1}{\Omega} \sum_{N_1=0}^N \int d\Omega_1 Z(N_1, \Omega_1, T) Z(N_2, \Omega_2, T), \quad (1)$$

where Z is the canonical partition function, the probability density for the coordinates $R = \{\mathbf{r}_1, \dots, \mathbf{r}_N\}$ of the particles, the number N_1 , and the volume Ω_1 can be cast in the form

$$P_{N,\Omega,T}(R, N_1, \Omega_1) \propto \frac{\Omega_1^{N_1+1} \Omega_2^{N_2+1}}{N_1! N_2!} e^{-\beta V(R)}. \quad (2)$$

^{a)}Electronic mail: rfantoni@ts.infn.it

^{b)}Electronic mail: moroni@democritos.it

Here, $\beta = 1/k_B T$ and the potential energy in the Boltzmann weight, assuming a central pair potential $v(r)$, is

$$V(R) = \sum_{i=1}^{N_1-1} \sum_{j=i+1}^{N_1} v(r_{ij}) + \sum_{i=N_1+1}^{N-1} \sum_{j=i+1}^N v(r_{ij}). \quad (3)$$

The Monte Carlo simulation proceeds via three kinds of moves:

(1) Displace the position \mathbf{r}_i of a randomly selected particle within its own box; this is done as in standard canonical ensemble simulations.

(2) Change the volumes; this is done by uniformly sampling a displacement of the quantity $\ln(\Omega_1/\Omega_2)$, with Ω kept fixed.

(3) Exchange particles; this is done by transferring a randomly chosen particle to a random position in the other box.

The acceptance probabilities are obtained imposing detailed balance.¹² After equilibration, provided N/Ω is within the coexistence region at the temperature T , each of the two boxes will contain one of the coexisting phases.

III. QUANTUM GIBBS ENSEMBLE MONTE CARLO

The QGEMC is based on the Path Integral Monte Carlo method in the Worm Algorithm implementation. We refer to the literature^{4,6} for a full account of these techniques, giving here only a brief discussion of some aspects relevant to the quantum generalization of the classical GEMC.

A. Path integral Monte Carlo

We consider an assembly of N identical particles obeying Bose statistics. In the position representation, the canonical partition function is

$$Z = \frac{1}{N!} \sum_{\mathcal{P}} \int dR \rho(R, \mathcal{P}R; \beta), \quad (4)$$

where $\rho(R, R'; \beta) = \langle R | e^{-\beta H} | R' \rangle$ is the thermal density matrix for distinguishable particles, and the sum over the permutations \mathcal{P} accounts for Bose symmetry. The density matrix can be expressed in a form amenable to Monte Carlo simulation in terms of discretized path integrals

$$\rho(R, R'; \beta) \simeq \int dR_1 \dots dR_{K-1} \prod_{j=1}^K \tilde{\rho}(R_{j-1}, R_j; \epsilon), \quad (5)$$

with $R_0 = R$, $R_K = R'$, and $\{R_1, \dots, R_{K-1}\}$ a sequence (path) of intermediate configurations. An adjacent pair $\{R_{j-1}, R_j\}$ is called a *link*. In Eq. (5), the factors $\tilde{\rho}$ have an argument $\epsilon = \beta/K$ which corresponds to a temperature K times higher than T , and for high temperature the unknown many-body density matrix can be accurately approximated by an explicit expression of the general form

$$\tilde{\rho}(R, R'; \epsilon) = \rho_F(R, R'; \epsilon) e^{-U(R, R'; \epsilon)}, \quad (6)$$

where

$$\rho_F(R, R'; \epsilon) = (4\pi\lambda\epsilon)^{-dN/2} \prod_{i=1}^N e^{-\mathbf{r}_i - \mathbf{r}'_i)^2 / 4\lambda\epsilon} \quad (7)$$

is the density matrix for N non-interacting particles in d spatial dimensions, and the function U takes into account the effect of correlations. In the limit $\epsilon \rightarrow 0$, $\tilde{\rho}(R, R', \epsilon)$ approaches $\rho(R, R', \epsilon)$ and the approximate equality (5) becomes exact.

For each particle, Eq. (5) defines a trajectory, or world line (WL), $\{\mathbf{r}_{i,0}, \mathbf{r}_{i,1}, \dots, \mathbf{r}_{i,K}\}$, where the *bead* $\mathbf{r}_{i,j}$ is the position of the i th particle at the j th “time” discretization index. In the calculation of thermal averages, $\langle A \rangle = \text{Tr} \rho A / Z$, the presence of the traces and the Bose symmetry of Eq. (4) require periodic boundary conditions in time, $\mathbf{r}_{i,K} = \mathbf{r}_{\mathcal{P}i,0}$: the trajectory of a particle ends in the initial position of either the same or another particle, according to the permutation cycles contained in the permutation \mathcal{P} . All the interlinked trajectories of a permutation cycle of k particles form a single WL with kK steps, so that all WLs are closed. The WL of a single particle has a spatial extent limited by the thermal wavelength, while the WL of a long permutation cycle can span the whole system.

The simulation proceeds by sampling a density probability proportional to the integrand of Eq. (5). Specific techniques are devised to update not only the particle positions along the WLs, but also the permutations.

The WLs can be mapped onto classical ring polymers, with peculiar interactions defined through Eq. (5) by viewing the integrand as a Boltzmann weight. Thus, it seems possible to apply the GEMC method to the quantum system as well. However, an issue arises with the exchange move: a quantum particle corresponds, in the classical mapping, to a whole polymer, and the acceptance rate for transferring a polymer to the other box can be expected to be low, particularly at low temperature when the thermal wavelength increases and the spatial extension of the polymers grows. The problem is further compounded by the presence of interlinked trajectories belonging to a permutation cycle. This is why quantum applications of GEMC have been limited to relatively high temperature and/or relatively low quantumness.¹¹ We will show how to overcome these difficulties using the WA.

B. Worm algorithm

The WA enlarges the configuration space: along with the closed WLs of Sec. III A, there are configurations with an open WL in which one particle is created in $\mathbf{r}_{\mathcal{M}}$ at time $j_{\mathcal{M}}\epsilon$ and destroyed in $\mathbf{r}_{\mathcal{I}}$ at a later time $j_{\mathcal{I}}\epsilon$. The difference $j_{\mathcal{I}} - j_{\mathcal{M}}$ is intended modulo K , and the open WL can belong to a permutation cycle involving other particles. The points $\mathbf{r}_{\mathcal{I}}$ and $\mathbf{r}_{\mathcal{M}}$ are called *Ira* and *Masha*, respectively, and the WL connecting them is called the *worm*. Configurations with only closed WLs belong to the “Z sector” and contribute to the partition function. Configurations with a worm belong to the “G sector” and contribute to the one-body Green function $g(\mathbf{r}_{\mathcal{M}}, \mathbf{r}_{\mathcal{I}}; (j_{\mathcal{I}} - j_{\mathcal{M}})\epsilon) / Z$. All physical properties, with the exception of the Green function, are calculated only on configurations of the Z sector. The full set of configurations corresponds to the extended partition function

$$Z_W = Z + Z', \quad (8)$$

where Z can be either the canonical or the grand partition function,

$$Z' = C \sum_{j_I, j_M} \int d\mathbf{r}_I d\mathbf{r}_M g(\mathbf{r}_M, \mathbf{r}_I; (j_I - j_M)\epsilon), \quad (9)$$

and the arbitrary parameter C defines the relative weight of the Z and G sectors. The discretized path integral expression of Eq. (9) is obtained in close analogy with Sec. III A in terms of $\tilde{\rho}(R_{j-1}, R_j; \epsilon)$.

The simulation proceeds via a set of local moves – the complementary pairs *Open* and *Close*, *Insert* and *Remove*, *Advance* and *Recede*, and the self-complementary *Swap* – which guarantee ergodic sampling of the enlarged configuration space by switching between the Z and the G sectors and displacing the coordinates of the particles.⁶

The usefulness of the WA for the implementation of the QGEMC can be appreciated by considering the process of adding a particle to the system (we assume here that Z is the grand partition function): starting from the Z sector, a worm may be *inserted*; once in the G sector, the worm may *advance*, possibly *swap* with existing closed WLs, and eventually get *closed*, thus switching back to the Z sector with one more particle. Each single move is a local update that involves only a limited number of time steps, so that the acceptance rate can be high even in a dense system.

C. Gibbs ensemble

We consider N_1 particles in a volume Ω_1 and N_2 particles in a volume Ω_2 , with Ω , N , and T fixed (see Sec. II). The configurations of the system in the Gibbs ensemble are distributed according to the partition function Z_G of Eq. (1), with each of the canonical partition functions Z of the two subsystems expressed as discretized path integrals with closed WLs, as in Sec. III A. These configurations define the Z sector.

Following the strategy of the WA we enlarge the configuration space allowing for open WLs, while strictly enforcing the constraint of fixed N : whenever there is a worm in box 1, with Masha at $\mathbf{r}_{M1;j}$ and Ira at $\mathbf{r}_{I1;j'}$, there is a worm in box 2 as well, with Masha at $\mathbf{r}_{M2;j'}$ and Ira at $\mathbf{r}_{I2;j}$, as schematically illustrated in Fig. 1. These configurations define the G sector. In the G sector, the number of particles in box α ($\alpha = 1, 2$) varies between N_α and $N_\alpha - 1$, with $N_1 + N_2 = N + 1$, and the total number of particles within each link is N .

The extended partition function is $Z_w = Z_G + Z'$, where

$$Z' = \frac{1}{\Omega} \sum_{N_1} \int d\Omega_1 C \sum_{j, j'=1}^K F_1(j, j') F_2(j', j). \quad (10)$$

The primed summation excludes the terms with $j = j'$ to make sure there is a worm per box in the G sector, and the function F_α – the integral of Eq. (9) for box α – is expressed in terms of density matrices as

$$F_\alpha(j, j') = \frac{1}{N_\alpha!} \sum_{\mathcal{P}_\alpha} \int \rho(\{R_\alpha, \mathbf{r}_{M\alpha}\}, \mathcal{P}_\alpha \{R'_\alpha, \mathbf{r}_{I\alpha}\}; \tau_{j, j'}) \times \rho(R'_\alpha, R_\alpha; \tau_{j', j}) dR_\alpha dR'_\alpha d\mathbf{r}_{M\alpha} d\mathbf{r}_{I\alpha}. \quad (11)$$

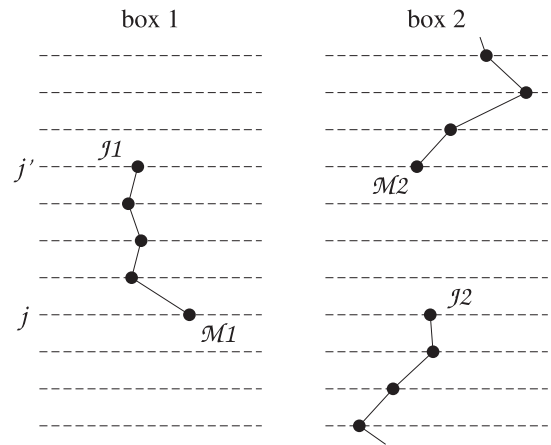


FIG. 1. Schematic illustration of open WLs in the G sector.

Here, the pair $\{R_\alpha, \mathbf{r}_{M\alpha}\}$ indicates the coordinates of Masha and of all the other particles of box α at time index j (the first argument of F_α) and $\{R'_\alpha, \mathbf{r}_{I\alpha}\}$ the coordinates of Ira and of the other particles at j' . The argument $\tau_{j, j'}$ of the density matrices ρ is the positive interval from $j\epsilon$ to $j'\epsilon$ – possibly wrapping around the periodic boundary condition, i.e., $\tau_{j, j'} = [(j' - j + K) \bmod K] \epsilon$. Finally, the density matrices are expanded in discretized path integrals using the high temperature approximation $\tilde{\rho}$ as in Sec. III A.

The probability density for all the coordinates X in the system, the number N_1 and the volume Ω_1 is¹³

$$P_{N, \Omega, T}(X) \propto C^{\delta_G} \prod_{j=1}^K \tilde{\rho}(X_{j-1}, X_j; \epsilon), \quad (12)$$

where δ_G is 1(0) in the $G(Z)$ sector, X_j indicates the positions of all the particles in either box at time $j\epsilon$, and the dependence on N_1 and Ω_1 , as well as all possible permutations of particle labels, are implicitly contained in the configuration X . No sums over permutations appear in P because the symmetrizations of Eq. (11) or (4) are carried out concurrently with the Monte Carlo integration over the coordinates, through updates of the permutation cycles.

We next describe a set of moves which sample the configuration space with probability density $P_{N, \Omega, T}(X)$. They are the standard moves of PIMC and the WA, in some cases combined in pairs to preserve the two-worm structure of the G sector illustrated in Fig. 1, and the volume change move specific of the GEMC method; the particles exchange move of GEMC builds spontaneously through a sequence of WA moves. The acceptance probabilities are obtained by enforcing detailed balance according to the generalized Metropolis algorithm¹² (if the current configuration is in a sector where the proposed move is not applicable, the move is rejected immediately).

(1a) *Open-insert*. This move, schematically illustrated in Fig. 2, is applicable only in the Z sector. It switches from the Z to the G sector by opening an existing closed WL in one box and inserting a new open WL in the other box. A particle is picked randomly, and the links of its WL from j to $j + M$ are removed. The time index j is uniformly sampled in $[1, K]$, and the number of removed links M is uniformly sampled in $[1, \bar{M}]$, where $\bar{M} < K$ is a parameter of the simulation which

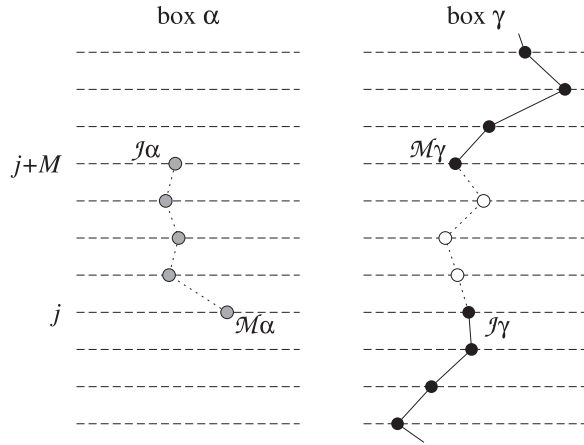


FIG. 2. Schematic illustration of the open-insert move. Two worms are created by removing the white beads and inserting the grey beads.

controls the size of the move. Let α be the label of the other box. The initial bead $\mathbf{r}_{M\alpha;j}$ of the new WL is placed at a position \mathbf{r}_0 randomly sampled in Ω_α , and M further beads are sampled from $\prod_{v=1}^M \rho_0(\mathbf{r}_{v-1}, \mathbf{r}_v; \epsilon)$, where

$$\rho_0(\mathbf{r}, \mathbf{r}'; \epsilon) = (4\pi\lambda\epsilon)^{-d/2} e^{-(\mathbf{r}-\mathbf{r}')^2/4\lambda\epsilon} \quad (13)$$

is the one-particle free propagator. The acceptance probability is $p_{\text{op-in}} = \min\{1, e^{\Delta_U} \pi_{\text{op-in}}\}$, where

$$\pi_{\text{op-in}} = \frac{C\bar{M}K\Omega_\alpha N}{2\rho_0(\mathbf{r}_{\mathcal{I}\gamma}, \mathbf{r}_{\mathcal{M}\gamma}; M\epsilon)} \quad (14)$$

and $\Delta_U = \sum_{v=1}^M [U(X_{v-1}, X_v; \epsilon) - U(X_{v-1}^*, X_v^*; \epsilon)]$ is the change of the interacting part of the action U between the initial configuration X and the proposed configuration X^* .

(1b) *Close-remove* is the complementary move of *open-insert*. A box – say γ – is selected at random. If $M = \tau_{\mathcal{I}\gamma, \mathcal{M}\gamma}/\epsilon > \bar{M}$, the move is rejected. Otherwise, a WL of M links connecting $\mathbf{r}_0 = \mathbf{r}_{\mathcal{I}\gamma}$ to $\mathbf{r}_M = \mathbf{r}_{\mathcal{M}\gamma}$ is sampled from $\prod_{v=1}^M \rho_0(\mathbf{r}_{v-1}, \mathbf{r}_v; \epsilon)$. If the open WL in the other box contains more than \bar{M} links the move is rejected, otherwise the worm is removed. The acceptance probability is $p_{\text{cl-rm}} = \min\{1, e^{\Delta_U}/\pi_{\text{op-in}}\}$.

(2) *Advance-recede*. This move is self-complementary, as are all the remaining moves. It applies only to the G sector, and we refer to Fig. 1 for a representation of the initial configuration. A box – say γ – is selected at random. An integer M is uniformly sampled in $[1, \bar{M}]$ and a time direction is selected at random. If the time direction is positive, a new portion of WL sampled from a product of M free-particle propagators is added in box γ starting from $\mathbf{r}_{\mathcal{I}\gamma}$, and a corresponding, M -link portion of the open WL existing in box α is removed, starting from $\mathbf{r}_{\mathcal{M}\alpha}$. If the time direction is negative, the new portion of WL is added in box γ starting from $\mathbf{r}_{\mathcal{M}\gamma}$ and going backwards in time, and the WL in box α is shortened starting from $\mathbf{r}_{\mathcal{I}\alpha}$. The move is rejected if $M \geq \tau_{\mathcal{I}\gamma, \mathcal{M}\gamma}/\epsilon$ (this restriction could be avoided using more elaborate combinations of the WA moves). The acceptance probability of *advance-recede* is $p_{\text{ad-re}} = \min\{1, e^{\Delta_U}\}$.

(3) *Swap*. This move applies only to the G sector. A box is selected at random, and within the chosen box the move proceeds in the same way as in the WA.⁶

(4) *Volume change*. We choose to apply this move only to configurations of the Z sector. For the classical GEMC update of the volumes, it proves convenient to make the dependence on N_1 and Ω_1 explicit. This is achieved¹² by rescaling all lengths in box α by $\Omega_\alpha^{-1/d}$ and formally performing the Monte Carlo integration over the rescaled coordinates $\Xi(X)$. Furthermore, the move is usually implemented¹² by changing the quantity $\ln(\Omega_1/\Omega_2)$, rather than Ω_1 itself, by an amount uniformly sampled in $[-\Delta_\Omega, \Delta_\Omega]$ with Δ_Ω a parameter which controls the size of the move. A factor $\Omega_1^{N_1} \Omega_2^{N_2}$ appears in $P_{N, \Omega, T}$ as a result of rescaling the coordinates, and another factor $\Omega_1 \Omega_2$ as a result of updating the logarithm of the volume (cf. Eq. (2)). In the quantum case, we adopt the same changes of variables. Since each particle is mapped onto K beads, each of which gets rescaled coordinates, the probability density is

$$P_{N, \Omega, T}(\Xi, N_1, \Omega_1) \propto \Omega_1^{KN_1+1} \Omega_2^{KN_2+1} \times \prod_j \tilde{\rho}(X_{j-1}(\Xi), X_j(\Xi); \epsilon). \quad (15)$$

The acceptance probability for a move from Ω_1 to Ω_1^* is

$$p_{\text{vol}} = \min \left\{ 1, \left(\frac{\Omega_1^*}{\Omega_1} \right)^{KN_1+1} \left(\frac{\Omega_2^*}{\Omega_2} \right)^{KN_2+1} e^{\Delta_S} \right\}, \quad (16)$$

where Δ_S is the change of the *full* action between the initial configuration X and the proposed configuration X^*

$$\Delta_S = - \sum_{v=1}^K \ln[\tilde{\rho}(X_{v-1}, X_v; \epsilon)/\tilde{\rho}(X_{v-1}^*, X_v^*; \epsilon)]. \quad (17)$$

The proposed configuration is $X^* = (\Omega_\alpha^*/\Omega_\alpha)^{1/d} X$, with $\alpha = 1$ or 2 as appropriate to the particle index of each component of X . Hence, both the equal-time interparticle distances, $|\mathbf{r}_{i;j} - \mathbf{r}_{k;j}|$, and the single-particle displacements along the WL, $|\mathbf{r}_{i;j-1} - \mathbf{r}_{i;j}|$, are modified upon volume changes. This prescription departs from that recommended for classical systems of composite particles,¹² where only the center of mass follows the variation of the volume while the internal structure remains unchanged (in the quantum analogue, only the centroid of each ring polymer would change while the size and shape of the polymers would stay fixed¹¹). The reason for the prescription chosen here is that for polymers interlinked through permutation cycles the equal-time interparticle distance and the single-particle paths are not independent.

In our implementation, we also include moves which *wiggle* an existing portion of a WL, or *displace* the whole WL of a particle. These moves are standard in PIMC⁴ and since they are not strictly needed for the QGEMC we do not describe them here.

IV. TWO-DIMENSIONAL ⁴He

The phase diagram of ⁴He in two dimensions has been studied in Ref. 14 by PIMC simulations of individual phases

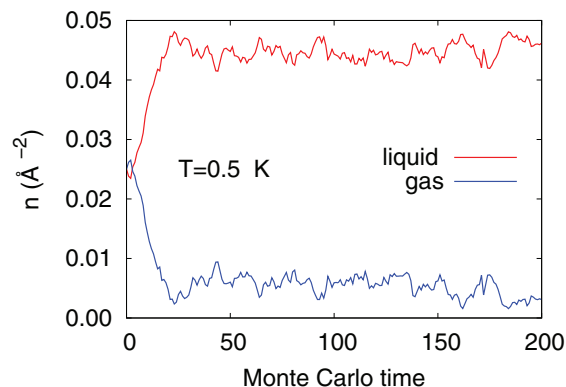


FIG. 3. Data trace of the densities of the gas (blue) and the liquid (red) in the initial stages of the simulation for $T = 0.5$ K.

for many values of density and temperature. A gas-liquid coexistence region is found below 0.87 K. At these temperatures, on account of the large De Boer parameter of ${}^4\text{He}$, $\Lambda = 0.429$,⁹ quantum exchange of particles is an important effect:^{4,8} in the thermodynamic limit the normal-superfluid transition temperature at saturated vapour pressure is 0.65 K,⁶ and for finite systems of a few hundred particles the superfluid fraction is non-zero even for $T = 1$ K. Therefore, the gas-liquid coexistence of two-dimensional ${}^4\text{He}$ is a telling test of the QGEMC algorithm for a degenerate quantum system. An application to a square well model and ${}^4\text{He}$ in three dimensions has also appeared.¹⁵

We simulate a two-dimensional system of $N = 64$ ${}^4\text{He}$ atoms distributed between two square boxes with periodic boundary conditions. Within each box, the atoms interact with the HFDHE2 pair potential.¹⁶ We use the primitive approximation

$$\tilde{\rho}(R, R'; \epsilon) = \rho_F(R, R'; \epsilon) e^{-\epsilon[V(R)+V(R')]/2} \quad (18)$$

to the high temperature density matrix, with $\epsilon = 0.002$ K⁻¹. The acceptance rate of the moves can be varied by tuning the relevant parameters. In this calculation, we set $\bar{M} = 125$, with acceptances between 35% and 75% for the close-remove, advance-recede, swap and wiggle moves, but only a few percent for the open-insert move. The acceptances of the volume move are between 20% and 40% with $\Delta_\Omega = 10^{-2}$, across the

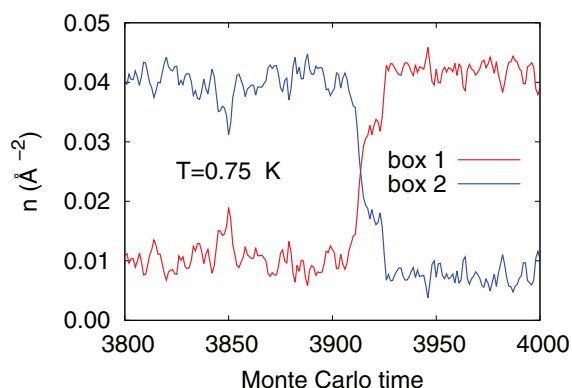


FIG. 4. A portion of the data trace of the densities for the simulation at $T = 0.75$ K, showing an exchange of identity between the two boxes.

TABLE I. The densities n_g and n_l of the coexisting gas and liquid phases as a function of the temperature T .

T (K)	n_g (\AA^{-2})	n_l (\AA^{-2})
	This work	
0.125	$< 10^{-6}$	0.0422(2)
0.250	0.00009(2)	0.0424(4)
0.500	0.0016(2)	0.0416(4)
0.750	0.0106(6)	0.0396(7)
0.875	0.0209(9)	0.0343(10)
	Ref. 14	
0.250	0.000(2)	0.044(2)
0.500	0.000(2)	0.044(2)
0.750	0.009(2)	0.043(2)
0.860	0.020(2)	0.030(2)

whole temperature range. We also adjust the parameter C to maintain the fraction of configurations in the Z sector between 0.15 and 0.55. In principle, a different value of \bar{M} should be used for each move, and all these parameters, as well as the relative frequency of the moves, should be optimized by maximizing the efficiency. We study the temperature range between 0.125 K and 1 K. For each temperature, the simulation starts from a configuration with boxes of equal volume containing 32 atoms each at a density 0.025 \AA^{-2} .

After equilibration, deep in the subcritical temperature regime one of the boxes contains a gas of very low density n_g , and the other a superfluid liquid with a density n_l close to the equilibrium density of the system at $T = 0$ (see Fig. 3). For temperatures closer to the critical point, n_g and n_l approach each other, and we frequently observe that the two boxes exchange identity, i.e., the phase of the system in each box switches back and forth between gas and liquid (see Fig. 4). In this case, the density has a bimodal distribution peaked at the values n_g and n_l of the coexisting phases. This bimodal distribution can be obtained in a grand canonical simulation of a single box, but this requires a fine tuning of the chemical potential.¹⁷ For $T = 1$ K, the two peaks merge into a single gaussian centered at the average density 0.025 \AA^{-2} .

Our results for the densities n_g and n_l of the coexisting phases are listed in Table I and displayed in Fig. 5. They compare favorably with the results of Ref. 14. For each T , the

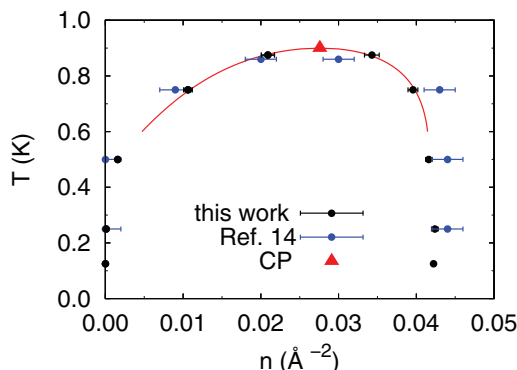


FIG. 5. The binodal line of ${}^4\text{He}$ in two dimensions. Black points: QGEMC. Blue points: Ref. 14. Red line: extrapolation of the QGEMC results to the critical point (red triangle).

TABLE II. The superfluid fraction n_s in the coexisting gas and fluid phases as a function of T .

T (K)	n_s	
	Gas	Liquid
1.000		0.032(1)
0.875	0.14(3)	0.36(2)
0.750	0.06(3)	0.63(3)
0.500	0.0014(5)	0.938(7)
0.250	$<10^{-3}$	0.963(10)
0.125	0	0.985(16)

latter are obtained from an integral of the isothermal pressure calculated in the canonical ensemble for several values of the density across the coexistence region; the QGEMC method is simpler because n_g and n_l are obtained with a single simulation, either directly or via the analysis of a bimodal distribution. Each of the present QGEMC calculations took ~ 300 CPU hours on a 2 GHz processor. If needed, the efficiency could be significantly improved using a better approximation to the high temperature density matrix.⁴

The boundary of the gas-liquid coexistence region is called the binodal line. It can be extrapolated to the critical point (CP) using the law of “rectilinear diameters,”¹⁸ $\rho_l + \rho_g = 2\rho_c + a|T - T_c|$, and the expansion¹⁹ $\rho_l - \rho_g = b|T - T_c|^{\beta_1}(|T - T_c| + c)^{\beta_0 - \beta_1}$. Here, $\beta_1 = 1/2$ and $\beta_0 = 1/8$, while ρ_c , T_c , a , b , and c are fitting parameters. We find $\rho_c = 0.028 \text{ \AA}^{-2}$ and $T_c = 0.90 \text{ K}$.

Finally, we list in Table II the winding number estimator⁸ of the superfluid fraction n_s for the two phases as a function of the temperature. A non-zero value on the liquid branch of the binodal over the full range of temperatures considered is a clear indication of the importance of quantum exchanges. On the gas branch of the binodal a finite superfluid fraction also appears, but only at $T \gtrsim 0.5 \text{ K}$, where the density begins to increase significantly entailing a corresponding increase of the degeneracy temperature (although, as mentioned, a finite value of n_s for $T > 0.65 \text{ K}$ is a finite size effect⁶).

V. CONCLUSIONS

We have presented the QGEMC method, a full quantum extension of classical Gibbs Ensemble Monte Carlo based

on the Worm Algorithm. The method is demonstrated for the binodal of ^4He in two dimensions, a physical property of a strongly quantum system in the degenerate temperature regime. Good agreement is found with the results of previous PIMC simulations in the canonical ensemble. In analogy with applications of GEMC to classical fluids,^{20–22} the QGEMC method offers a convenient approach for problems such as gas-liquid coexistence in quantum systems and phase equilibria in quantum mixtures.

ACKNOWLEDGMENTS

We are grateful to M. E. Fisher for correspondence and helpful comments.

- ¹M. H. Kalos and P. A. Whitlock, *Monte Carlo Methods* (Wiley-VCH Verlag GmbH & Co. KGaA, Weinheim, 2008).
- ²A. Z. Panagiotopoulos, *Mol. Phys.* **61**, 813 (1987); B. Smit, Ph. De Smedt, and D. Frenkel, *ibid.* **68**, 931 (1989); B. Smit and D. Frenkel, *ibid.* **68**, 951 (1989).
- ³R. P. Feynman, *Rev. Mod. Phys.* **20**, 367 (1948).
- ⁴D. M. Ceperley, *Rev. Mod. Phys.* **67**, 279 (1995).
- ⁵D. M. Ceperley, *J. Stat. Phys.* **63**, 1237 (1991).
- ⁶M. Boninsegni, N. V. Prokof'ev, and B. V. Svistunov, *Phys. Rev. Lett.* **96**, 070601 (2006); *Phys. Rev. E* **74**, 03670 (2006).
- ⁷N. V. Prokof'ev, B. V. Svistunov, and I. S. Tupitsyn, *Phys. Lett. A* **238**, 253 (1998); *JETP* **87**, 310 (1998).
- ⁸E. L. Pollock and D. M. Ceperley, *Phys. Rev. B* **36**, 8343 (1987).
- ⁹R. A. Young, *Phys. Rev. Lett.* **45**, 638 (1980).
- ¹⁰F. Schneider, D. Marx, and P. Nielaba, *Phys. Rev. E* **51**, 5162 (1995); P. Nielaba, *Int. J. Thermophys.* **17**, 157 (1996).
- ¹¹Q. Wang and J. K. Johnson, *Fluid Phase Equilib.* **132**, 93 (1997); I. Georgescu, S. E. Brown, and V. A. Mandelshtam, *J. Chem. Phys.* **138**, 134502 (2013); P. Kowalczyk, P. A. Gauden, A. P. Terzyk, E. Pantatosaki, and G. K. Papadopoulos, *J. Chem. Theory Comput.* **9**, 2922 (2013).
- ¹²D. Frenkel and B. Smit, *Understanding Molecular Simulation* (Academic Press, San Diego, 1996), Appendix G.
- ¹³The link density matrix $\tilde{\rho}(X, X'; \epsilon)$ of the whole system is the product $\tilde{\rho}(R_\alpha, R'_\alpha; \epsilon)\tilde{\rho}(R_\gamma, R'_\gamma; \epsilon)$ over the two boxes; particle labels are only permuted within each box.
- ¹⁴M. C. Gordillo and D. M. Ceperley, *Phys. Rev. B* **58**, 6447 (1998).
- ¹⁵R. Fantoni, *Phys. Rev. E* **90**, 020102(R) (2014).
- ¹⁶R. A. Aziz, V. P. S. Nain, J. S. Carley, W. L. Taylor, and G. T. McConville, *J. Chem. Phys.* **70**, 4330 (1979).
- ¹⁷N. B. Wilding, *Phys. Rev. E* **52**, 602 (1995).
- ¹⁸E. A. Guggenheim, *J. Chem. Phys.* **13**, 253 (1945).
- ¹⁹M. E. Fisher, *Phys. Rev. Lett.* **16**, 11 (1966).
- ²⁰R. Fantoni, A. Malijeviský, A. Santos, and A. Giacometti, *Europhys. Lett.* **93**, 26002 (2011).
- ²¹R. Fantoni, A. Giacometti, M. A. G. Maestre, and A. Santos, *J. Chem. Phys.* **139**, 174902 (2013).
- ²²R. Fantoni and G. Pastore, *Phys. Rev. E* **87**, 052303 (2013).